PAPER

Check for updates

Preparation of nanoemulsions from *Elsholtzia kachinensis* and *Elsholtzia ciliata* essential oils *via* ultrasonic homogenization and their antibacterial and anticancer activities†

Nguyen Quang Tinh,[a] Dang Van Thanh, [ID][b] Nguyen Van Thu,[b] Bui Thi Quynh Nhung,[b] Pham Ngoc Huyen,[b] Nguyen Phu Hung,[c] Nguyen Thi Thuy, [ID][de] Pham Dieu Thuy,[a] Nguyen Hoa Mi[f] and Khieu Thi Tam [ID] *[g]

Plant essential oils can function as effective antibacterial and anticancer agents, but their low solubility and hydrophobic nature limit their practical applications. In this study, we report the preparation of nanoemulsions of *Elsholtzia kachinensis* and *Elsholtzia ciliata via* ultrasonic homogenization and the characterization of their antibacterial and anticancer activities for the first time. The product characteristics were evaluated based on turbidity, droplet size, polydispersion index, zeta potential and electrophoretic mobility. The activities were evaluated based on their ability to inhibit the growth of bacteria and HepG2 cancer cells. The *Elsholtzia kachinensis* and *Elsholtzia ciliata* nanoemulsions exhibited good stabilities, narrow size distributions with droplet sizes of 72.81 nm and 32.13 and zeta potentials of −27.8 mV and −11.2 mV, respectively. The Mulliken atomic charge analysis demonstrated that the *E. kachinensis* nanoemulsion had greater stability than the *E. ciliata* nanoemulsion. *In vitro* antibacterial studies using strains of *Escherichia coli*, *Pseudomonas aeruginosa*, *Klebsiella pneumoniae*, *Staphylococcus aureus*, *Bacillus subtilis* and *Staphylococcus epidermidis* showed that both nanoemulsions exhibited higher growth inhibition efficiency than the respective essential oils. The inhibition efficiency of the *Elsholtzia ciliata* nanoemulsion against *Bacillus subtilis* and *Staphylococcus epidermidis* was 5 times higher than those of the corresponding essential oils. The HepG2 cell inhibition efficiency was about 80% for both nanoemulsions at a concentration of 500 μg mL^{-1}, while the commercial essential oils inhibited only about 60% of HepG2 cells. Therefore, *Elsholtzia kachinensis* and *Elsholtzia ciliata* nanoemulsions can be potential candidates for modern biopharmaceuticals in the future.

1 Introduction

Elsholtzia, an important genus of aromatic herbs with a total of 42 species, is widely distributed all over the world and used in folk medicine to treat respiratory infectious diseases, such as fever, pneumonia and cold.[1,2] Some species in this genus are renowned for their essential oils, which possess various aromatic and medicinal properties.[2] The essential oils of *Elsholtzia* species typically contain a range of volatile compounds, such as aliphatic compounds, terpenoids and aromatic compounds, of which terpenoids are the main components.[3–5] The compositions of the essential oils of *Elsholtzia* species depend on the distribution of the species and the plant part used. Reports indicate that their essential oils possess a range of pharmacological activities with antibacterial, antioxidant, anti-inflammatory, and anticancer properties.[3–5] For example, these essential oils are considered key antibacterial components, with strong inhibitory effects on *Escherichia coli* (*E. coli*), *Pseudomonas aeruginosa* (*P. aeruginosa*), *Klebsiella pneumoniae* (*K. pneumoniae*) and *Staphylococcus aureus* (*S. aureus*).[6,7] *Elsholtzia kachinensis* (*E. kachinensis*) and *Elsholtzia ciliata* (*E. ciliata*) are two species that belong to the *Elsholtzia* genus. *E. kachinensis* with notable aromatic and medicinal qualities is used to support digestion and alleviate symptoms of bloating and pain.[8] The essential oils of this species mainly

[a]Thai Nguyen University of Agriculture and Forestry, Thai Nguyen 25000, Vietnam

[b]Thai Nguyen University of Pharmacy and Medicine, Thai Nguyen 25000, Vietnam

[c]Center for Interdisciplinary Science and Education, Thai Nguyen University, Tan Thinh Ward, Thai Nguyen 25000, Vietnam

[d]School of Chemical and Environmental Engineering, International University, Quarter 6, Linh Trung Ward, Thu Duc City, Ho Chi Minh City, Vietnam

[e]Vietnam National University Ho Chi Minh City, Linh Trung Ward, Thu Duc City, Ho Chi Minh City, Vietnam

[f]Center for Computational Chemistry, Faculty of Chemistry, VNU University of Science, 19 Le Thanh Tong, Hoan Kiem, Hanoi City, Vietnam

[g]Faculty of Chemistry, TNU-University of Sciences, Tan Thinh Ward, Thai Nguyen 25000, Vietnam. E-mail: tamkt@tnus.edu.vn

† Electronic supplementary information (ESI) available. See DOI: https://doi.org/10.1039/d5ra00386e

contain carvone and dehydroelsholtzia ketone, which have inhibitory effects against *S. aureus* and *Salmonella enterica*.[8] In addition, these essential oils are effective against insects, and hence, they have the potential to be developed into environmentally friendly pesticides.[8] *E. ciliata* is a popular species that is distributed widely all over the world. Previous studies on the volatile oils extracted from this species have shown that dehydrogenanone and elsholtzia ketone are the main components.[3,9] However, applications of these essential oils are limited due to issues, such as low stability, poor water solubility and susceptibility to oxidation.[10,11]

To overcome these limitations, essential oils can be formulated into nanoemulsions, which offer improved stability, increased surface area, and solubility and controlled release of their components, thereby increasing their biological efficacy.[12–15] Nanoemulsions maintain the quality of essential oils over time by protecting them from degradation and oxidation, improving their solubility and enabling the controlled release of their constituent compounds.[16] Moreover, the small droplet sizes of nanoemulsions increase the surface area for interactions and allow essential oils to reach deeper cell membranes, thereby increasing their biological efficacy.[12,13] As a result, nanoemulsions of essential oils exhibit higher bioactivity than the parent essential oils. Therefore, nanoemulsions offer a promising platform for enhancing the biological activity of essential oils by improving their characteristics. Various studies have demonstrated that incorporation of essential oils as nanoemulsions can enhance their antimicrobial and anticancer activities.[17–19] However, up to date, there are no reports on nanoemulsions of *E. kachinensis* and *E. ciliata* essential oils.

This study reports, for the first time, the preparation and characterization of nanoemulsions of *E. kachinensis* and *E. ciliata* essential oils. Additionally, the mechanism of nanoemulsion formation is proposed. Moreover, the antibacterial activities of these nanoemulsions against strains of Gram-negative (*E. coli*, *P. aeruginosa*, and *K. pneumoniae*) and Gram-positive (*S. aureus*, *B. subtilis*, *S. epidermidis*) bacteria were examined and compared with their corresponding essential oils. Finally, the anticancer activities of the nanoemulsions were investigated using the 3-(4,5-dimethylthiazolyl-2)-2,5-diphenyltetrazolium bromide (MTT) assay.

2 Methods

2.1 Materials

All chemicals, including *n*-hexane ($\geq$99%), Na_2SO_4 ($\geq$99%), and Tween 80 (99%) were purchased from Merck Chemicals. Fresh *E. kachinensis* was collected from Cao Bang Province, Vietnam (22°71′9.54″ N, 106°33′9.39″ E), and *E. ciliata* was obtained from Thai Nguyen Province, Vietnam (21°55′9.17″ N, 105°83′5.14″ E) in April 2024.

2.2 Extraction of essential oils from *E. kachinensis* and *E. ciliata*

Essential oils from the aerial parts of *E. kachinensis* (EKEO) and *E. ciliata* (ECEO) were extracted using the steam distillation method

using the Clevenger apparatus. Ten kilograms of *E. kachinensis* or *E. ciliata* were washed with distilled water, then chopped into small pieces and subjected to distillation. The *E. kachinensis* or *E. ciliata* samples were placed in the distillation apparatus, and water was added to submerge the samples. The obtained essential oils of *E. kachinensis* and *E. ciliata* were removed from the water using Na_2SO_4. The essential oils were stored at 4 °C for analyzing their chemical compositions, identifying their bioactivities and synthesizing their nanoemulsions.

2.3 Analysis of chemical constituents of essential oils using gas chromatography/mass spectra (GS/MS)

The chemical compositions of the essential oils were analysed using an Agilent 7890A gas chromatograph coupled with an Agilent MSD5975C mass spectrometer equipped with an HP-5MS fused silica capillary column (60 m × 0.25 mm *x* 0.25 μm). Helium was applied as the carrier gas at a flow rate of 1.0 mL min^{-1}. One microliter of the essential oil was diluted to a ratio of 1 : 50 with *n*-hexane and injected manually such that the flow ratio was 1 : 100. The temperature of the oven was initially set at 60 °C for 5 min, then heated gradually to 240 °C at the rate of 4 °C min^{-1} and was kept constant for 10 min. The temperature of the detector and interface was 270 °C. The mass spectra were recorded at 70 eV in the spectral range of 35–450 Da at 1.0 scan per s. The identification of essential oil constituents was carried out based on retention indices (RI) and the comparison of their mass spectra in the spectrogram library.[20] Essential oil components were reported in the form of relative concentrations of each peak area per total area in the gas chromatogram.

2.4 Preparation of *E. kachinensis* and *E. ciliata* nanoemulsions

The nanoemulsions of *E. kachinensis* (EKNE) and *E. ciliata* essential oils (ECNE) were prepared according to the method described by X. Fu *et al.*,[13] with slight modifications to obtain nanoemulsions with droplet sizes below 100 nm, narrow distributions, and good stabilities. According to X. Fu, Tween 80 is a suitable surfactant for the preparation of stable nanoemulsions. Tween 80 (15% (w/w)) and essential oils (10% (w/w)) were mixed until homogeneous using a magnetic stirrer at 1000 rpm for 15 min. Distilled water was then added dropwise to the mixture at a rate of 1 mL min^{-1} while stirring continuously at 800 rpm for 10 min. The mixture was then made up to a total volume of 50 mL using distilled water and subjected to ultrasonic treatment for 15 min at 2 kHz and 300 W operation power using an ultrasonic homogenizer (Scientz, Ningbo Xinzhi Biotechnology, China). The turbidity of the obtained nanoemulsions were measured and stored at 4 °C for 0 and 30 days in order to determine their droplet sizes, dispersion indexes, and zeta potentials. Their FTIR spectra and bioactivities were also evaluated. Fig. 1 displays the schematic representation of the synthesis of *E. kachinensis* and *E. ciliata* nanoemulsions.

2.5 Characteristics of the nanoemulsions

The optical density absorption of the nanoemulsions was measured at 600 nm using a UV-Vis spectrophotometer (Double
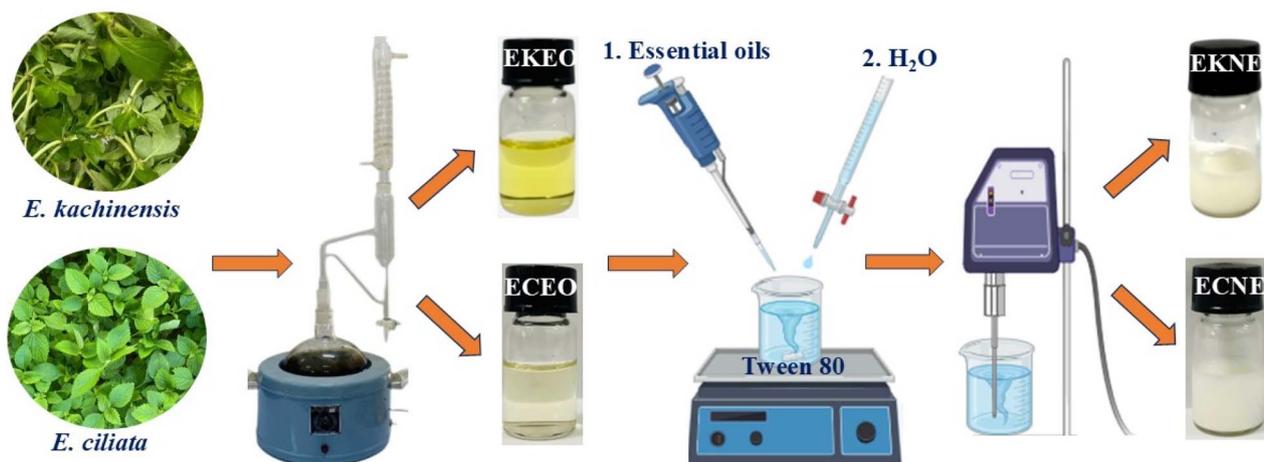
Fig. 1 Schematic for the synthesis of *E. kachinensis* and *E. ciliata* nanoemulsions.

Beam Spectrophotometer UH5300). The turbidity values of the nanoemulsions were calculated as follows:[21]

$$T = (2.023 \times A)/L$$

where T is turbidity (cm^{-1}), A is the absorbance at the λ_{max} of 600 nm, and L is the path length of the cuvette (cm).

The droplet size, polydispersion index (PDI), zeta potential and electrophoretic mobility of the nanoemulsions were determined using dynamic light scattering (DLS) (Horiba SZ-100, Japan) in the particle size measurement range of 0.3 nm to 10 μm and zeta potential range from −500 to +500 mV. The nanoemulsions were diluted to a 1 : 50 ratio with distilled water before measurement. The compositions of the nanoemulsions were identified using FTIR (Perkin Spectrum Two, Japan) by scanning in the wavenumber range of 4000–450 cm^{-1}.

2.6 Bioactivity

2.6.1 Antibacterial activity. The antibacterial activity of the essential oils and their nanoemulsions was evaluated using the agar disc diffusion method and the broth microdilution method. The agar disc diffusion method, a common method used to test bacterial susceptibility to antibiotics,[22] was applied in this study to measure the antibacterial activity of the samples against Gram-negative (*P. aeruginosa* from ATCC 27853) and Gram-positive (*S. aureus* from ATCC 25927) bacteria. Typically, 100 μL of the bacteria suspension at a concentration of 10^8 CFU mL^{-1} was spread on each agar plate. Six wells of diameter 6 mm were drilled in these plates. Then, 50 μL each of the four samples at an essential oil concentration of 10 mg mL^{-1}, 15% Tween 80 as the negative control and 4 μg per mL ciprofloxacin as the positive control were added to these wells, respectively, and incubated at 37 °C for 24 h. The inhibition zones were measured to determine the antibacterial ability of the samples. In the next step, the broth microdilution method was used to determine the minimum inhibitory concentration (MIC).[22] The minimum inhibitory concentrations of the samples against different strains of Gram-negative (*E. coli* (ATCC 25922), *P.*

aeruginosa (ATCC 27853), *K. pneumoniae* (ATCC 700603)) and Gram-positive (*S. aureus* (ATCC 25927), *B. subtilis* (ATCC 6633), *S. epidermidis* (ATCC 1228)) bacteria were determined using this method. The samples were diluted in dimethyl sulfoxide (DMSO) to produce solutions with a concentration of 7.5 mg essential oil per mL and 11.25 mg Tween 80 per mL^{-1}. Then, 100 μL of these samples were sequentially diluted in a 96 well plate containing 100 μL of Mueller–Hinton Broth (MHB) medium to produce a concentration range of 0.005–1.875 mg mL^{-1}. Finally, 100 μL of the respective bacterial suspension was added to the medium and incubated at 37 °C for 24 h. Ciprofloxacin was used in the concentration range of 0.0015–1 μg mL^{-1} as the reference antibiotic. The identified MIC values were the lowest concentration of samples at the well, which completely inhibited the growth of microorganisms. Each experiment was repeated three times.

2.6.2 Anticancer activity. The anticancer activity of the essential oils and nanoemulsions of *E. kachinensis* and *E. ciliata* against HepG2 liver cancer cells was evaluated using the MTT assay, as described in previous studies.[23,24] For this, 100 μL of HepG2 cells (5×10^3 cells per well) was cultured in a 96-well microplate using RPMI 1640 medium supplemented with 10% fetal bovine serum (FBS) and 1% penicillin/streptomycin. The plate was incubated for 48 h at 37 °C in a humidified atmosphere with 5% CO_2 and 95% O_2. After initial incubation, the HepG2 cells in the wells were exposed to the test samples at different concentrations (500, 200, 100, 50, 10, and 0 μg mL^{-1}). The control wells were treated with DMSO, while the blank wells contained only the culture medium. 5-Fluorouracil (5-FU), a cancer cell inhibitor, was used as the positive control at a concentration of 100 μM. The plate was incubated for 48 h under the same conditions (37 °C, 5% CO_2, and 95% O_2) to evaluate the impact of the samples on cell proliferation. To assess cell viability, 100 μL of fresh culture medium containing 10% MTT (5 mg mL^{-1}) was added to each well. The plate was incubated at 37 °C for 4 h and protected from light. After that, the MTT-containing medium was removed, and 100 μL of DMSO was added to each well to dissolve the formazan crystals.

The plate was shaken for 15 min. The cell proliferation rate was determined based on absorbance measurement at 570 nm using a Thermo Fisher Multiskan Sky Microplate Spectrophotometer. The images of the cells were captured prior to MTT analysis using an inverted microscope TS2 (Nikon, Japan) at 400× magnification. The percentage of cell proliferation was calculated using the following formula:

$$\% \text{ Cell proliferation} = (\text{OD}_{\text{treated samples}}/\text{OD}_{\text{control}}) \times 100$$

The IC$_{50}$ values, which represent the concentration of the sample that inhibits 50% cell growth, were calculated based on the optical density data and analyzed using the GraphPad Prism 5.0 software. The Mann–Whitney test was employed to identify the statistical significance of the data. Each experiment was repeated 3 times.

2.7 Computational investigations

Complementing the experimental findings, computational analysis was performed to explain the stability of nano-emulsions by evaluating their electrostatic interactions and zeta potentials. The geometrical structures and Mulliken atomic charges of molecules, including Tween 80, dehydroelsholtzia, *trans*-β-ocimene, and β-farnesene, were optimized at the B3LYP/6-31G* level. All computations were implemented using the Gaussian 16 software package.[25]

3 Results and discussion

3.1 Chemical compositions of the *E. kachinensis* and *E. ciliata* essential oils

The essential oils of *E. kachinensis* and *E. ciliata* were obtained by steam distillation with yields of 0.015% and 0.036%, respectively, compared with the weights of fresh samples. The results of the compositional analysis of *E. kachinensis* and *E. ciliata* essential oils are shown in Table S1,† Fig. 2a and b. Clearly, 36 compounds were identified in the essential oils of *E. kachinensis* and *E. ciliata*, representing 99.6% and 99.9% of their total compositions, respectively.

The major components of the *E. kachinensis* essential oil included dehydroelsholtzia ketone (62.86%), D-limonene (6.75%), β-caryophyllene (5.42%), 1-octen-3-ol-acetate (4.8%), and α-humulene (4.4%). The structures of these compounds are shown in Fig. 3. However, 36 components accounting for 98.767% of its composition were identified in the essential oil of
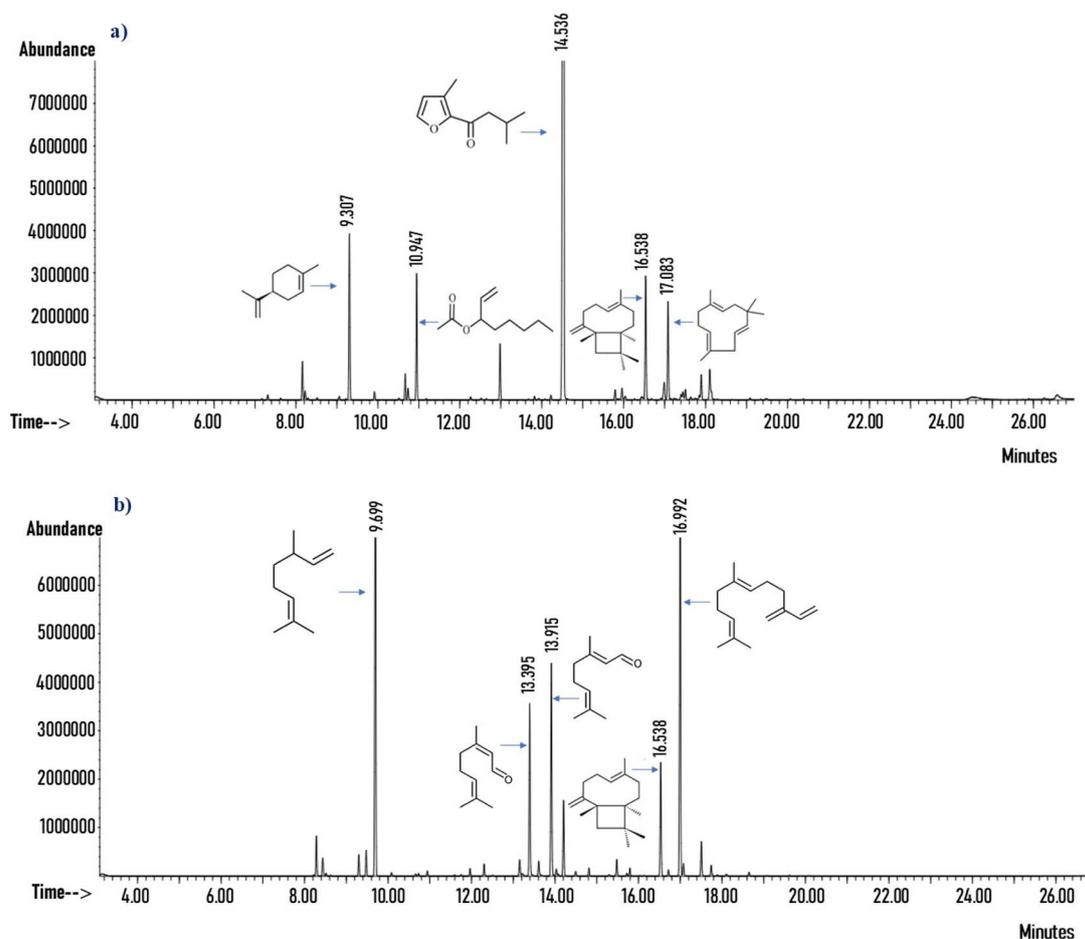

Fig. 2 GC/MS spectra of the essential oils of (a) *E. kachinensis* and (b) *E. ciliata*.
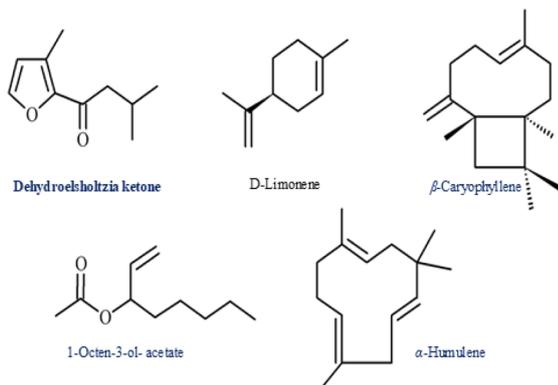
Fig. 3 Structures of the chemical components of the *E. kachinensis* essential oil.

this species harvested from Yunnan Province, China, with carvone (32.298%), dehydroelsholtzia ketone (31.540%), *E*-β-farnesene (10.098%), [2,2-dimethyl-4-(3-methylbut-2-enyl)-6-methylidenecyclohexyl]methanol (4.781%) and 1-octen-3-ol-acetate (4.123%)[8] as major constituents. While the main compounds of *E. ciliata* were *trans*-β-ocimene (29.21%), β-farnesene (24.25%), α-citral (11.15%), β-citral (8.99%) and β-caryophyllene (6.24%). The structures of these compounds are presented in Fig. 4. These components are distinct from those reported in previous works. For example, β-farnesene (10.8–11.7%), neral (15.2–20.5%), geranial (19.5–26.5%) and D-limonene (10.9–14.2%) were the major constituents of *E. ciliata* essential oils extracted from samples in south Vietnam,[26] whereas dehydroelsholtzia ketone (71.34%) and elsholtzia ketone (24.94%) were the main components of *E. ciliata* essential oils from Vilnius, Lithuania.[3] These differences in the essential oil components could be the result of factors such as location, climate, harvesting time and extraction method.[27] As a result, the quality and bioactivities of these essential oils may vary. Furthermore, previous studies have shown that most of the compounds in both essential oils possess promising therapeutic effects. Dehydroelsholtzia ketone, a terpene ketone, demonstrates inhibitory effects on various cancer cells, indicating its potential use for cancer treatment.[3] β-Caryophyllene is
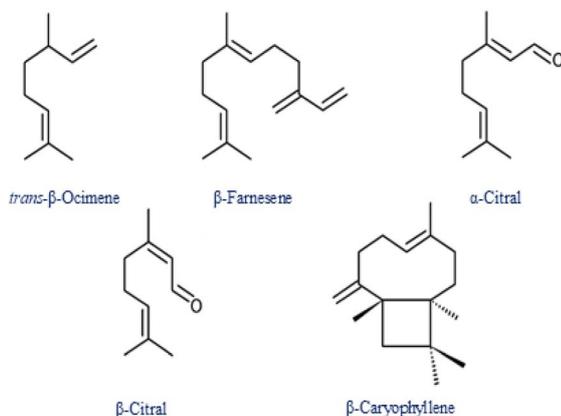
a natural compound with significant anticancer activity against several cancer cell types, and it can induce apoptosis and inhibit the growth of cancer cells.[28,29] These compounds are capable of donating electrons to free radicals, neutralizing their reactivity and preventing them from causing oxidative damage to cells. In addition, α and β-citral and monoterpenes, exhibit notable antibacterial, antioxidant and anticancer activities,[30,31] while ocimene shows cytotoxic effects against cancer cells, as well as antibacterial properties against various pathogens.[32] Therefore, the essential oils of *E. kachinensis* and *E. ciliata* exhibit great application scope in medicinal and pharmaceutical fields. However, it is necessary to formulate these oils into nano-emulsions for practical applications due to the poor solubility and stability of these essential oils.

## 3.2 Characteristics of the nanoemulsions of essential oils

The characteristics of nanoemulsions of essential oils are influenced by factors, such as the chemical composition of the essential oil, the surfactant used and the synthesis method.[16] Among surfactants, Tween 80 and Tween 20 are commonly used in the synthesis of essential oil-based nanoemulsions as they provide high stability, simplicity and safety without the need for a co-surfactant. Furthermore, Tween 80 has been demonstrated to be effective and is considered the optimal choice for achieving nanoemulsions with desired properties.[16] Thus, in the current study, Tween 80 was selected as the surfactant for the preparation of *E. kachinensis* and *E. ciliata* nanoemulsions. Ultrasonic homogenization is one of the most efficient techniques for preparing nanoemulsions from essential oils.[16] Thus, in this study, ultrasonic homogenization was used for the preparation of nanoemulsions. Additionally, the composition of the essential oil plays a crucial role in determining the stability and properties of the nanoemulsion, as different chemical constituents in the oil can interact with the surfactant and aqueous phase in different ways, influencing droplet size, stability, and polydispersity. Thus, the selection of essential oils with appropriate chemical profiles in conjunction with Tween 80 is key to the successful formation and stabilization of nanoemulsions.

In this study, the nanoemulsions of *E. kachinensis* and *E. ciliata* were synthesized using Tween 80 as the surfactant. The characteristics of these nanoemulsions, including turbidity, average drop size, polydispersity, zeta potential and electrophoretic mobility, were identified, as given in Table 1. Since the turbidity of a nanoemulsion is an important parameter for identifying its quality and stability, monitoring this parameter can be useful for optimizing the formulation for intended applications. As seen in Table 1, the turbidity of the *E. kachinensis* nanoemulsion was higher than that of the *E. ciliata* nanoemulsion, resulting in stronger light scattering. This result is consistent with their average droplet sizes given in Fig. 5. Accordingly, the average droplet size of the *E. kachinensis* nanoemulsion was larger compared to that of the *E. ciliata* nanoemulsion, which may be due to the chemical composition of the essential oils. Dehydroelsholtzia ketone is the major component of the *E. kachinensis* essential oil with larger polarity

Fig. 4 Structures of chemical components of the *E. ciliata* essential oil.

Table 1 Turbidity, average drop size, polydispersity, zeta potential and electrophoretic mobility of the nanoemulsions ($n = 3$)

Sample	Storage time (days)	Turbidity (cm^{-1})	Average drop size (nm)	Polydispersity	Zeta potential (mV)	Electrophoretic mobility (cm^2 V^{-1} s^{-1})
E. kachinensis nanoemulsion	0	1.757 ± 0.765	72.81 ± 2.12	0.281 ± 0.023	-27.8 ± 0.9	$-0.000215 \pm (-1.52 \times 10^{-6})$
	30	1.654 ± 0.546	95.16 ± 3.25	0.189 ± 0.015	-20.1 ± 1.2	$-0.000155 \pm (-1.34 \times 10^{-6})$
E. ciliata nanoemulsion	0	1.525 ± 0.643	32.13 ± 1.65	0.336 ± 0.042	-11.2 ± 0.7	$-0.000087 \pm (-0.98 \times 10^{-6})$
	30	1.456 ± 0.651	73.05 ± 1.89	0.231 ± 0.035	-7.9 ± 0.8	$-0.000061 \pm (-1.00 \times 10^{-6})$
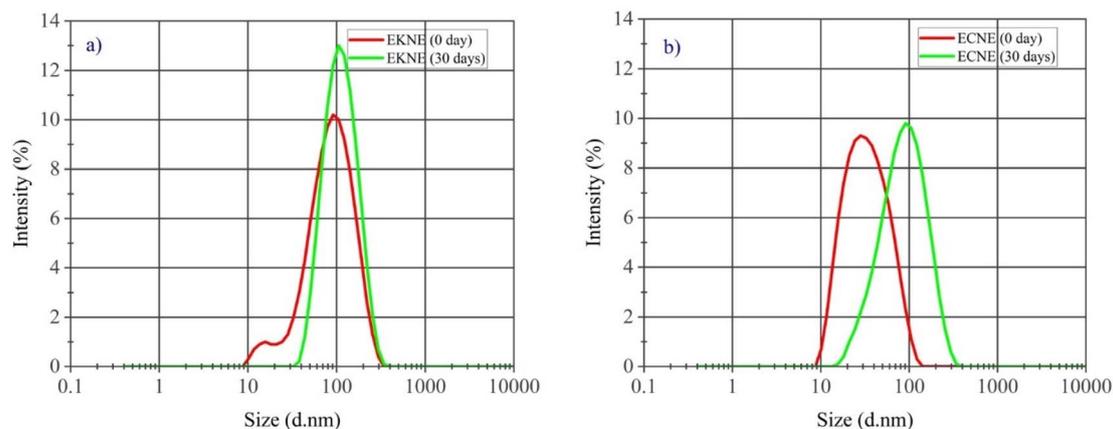
Fig. 5 Size distribution based on the DLS intensity of (a) *E. kachinensis* nanoemulsion and (b) *E. ciliata* nanoemulsion.

and molecular weight than monoterpenes, such as *trans*-β-ocimene and β-farnesene found in the *E. ciliata* essential oil, leading to the formation of larger droplets. This result is in agreement with previous reports,[33,34] which suggested that compounds with higher molecular weight tend to form larger sizes.

We further considered the PDI value, which is a dimensionless indicator of the size distribution of droplets. Typically, a low PDI value (<0.3) signifies a narrow size distribution, whereas values above 0.7 indicate a broad size distribution.[35] In this study, the PDI value of *E. kachinensis* (0.281) was lower than that of *E. ciliata* (0.336), which indicates a narrow size distribution in the *E. kachinensis* nanoemulsion. This is possibly due to the dominance of dehydroelsholtzia ketone in the *E. kachinensis* essential oil, resulting in a more uniform droplet size distribution in its nanoemulsion compared with that of the *E. ciliata* nanoemulsion. Since zeta potential is a main factor that represents the electrical charge of particles and defines the stability of nanoemulsions, this parameter was also monitored. The results showed that both nanoemulsions displayed negative zeta potential values, probably due to the non-ionic surfactant (Tween 80) and the negative charge of the essential oils. The ionization of hydroxyl groups in Tween 80 during dispersion into the medium and the presence of terpene in the essential oils may have contributed to the negative zeta potential values. In previous studies, nanoemulsions of the essential oils of eugenol,[13] garlic,[12] and green tea[18] prepared with Tween 80 have also shown negative zeta potential values. In addition, the *E. kachinensis* nanoemulsion had a significantly higher absolute zeta potential value (−27.8 mV) than that of the *E.*

ciliata nanoemulsion (−11.2 mV) (Fig. 6), suggesting that the *E. kachinensis* nanoemulsion was more stable.

The electrophoretic mobilities of the *E. kachinensis* and *E. ciliata* nanoemulsions were −0.000215 and −0.000087 cm^2 V^{-1} s^{-1}, respectively. These results indicate that the *E. kachinensis* nanoemulsion had greater stability, more uniform particle size distribution and less aggregation than the *E. ciliata* nanoemulsion. These findings align with the results of PDI and zeta potential mentioned above.

The stability of nanoemulsions is critical for their applications. Key parameters, including droplet size, PDI and zeta potential, are commonly utilized to examine nanoemulsion stability. In this study, these parameters were measured at the beginning (0 days) and after 30 days of storage at 4 °C. As shown in Table 1, Fig. 5, and 6, the droplet sizes of both *E. kachinensis* and *E. ciliata* nanoemulsions exhibited an increase over the storage period of 30 days, rising from 72.81 to 95.16 nm and 32.13 to 73.05 nm, respectively. This is possibly due to coalescence or Ostwald's ripening, which is an issue observed in oil-in-water emulsions.[36,37]

In the aqueous phase, oil molecules surrounding smaller droplets generally demonstrate greater water solubility than those surrounding larger droplets.[36,37] Consequently, oil molecules can be transferred from smaller to larger droplets, resulting in an increase in droplet size. However, despite this increase, the droplet sizes of the *E. kachinensis* and *E. ciliata* nanoemulsions remained below 100 nm. Furthermore, the turbidity, PDI, zeta potential values and electrophoretic mobilities of both nanoemulsions decreased after 30 days of storage. The PDI values decreased from 0.281 to 0.189 for the *E.*
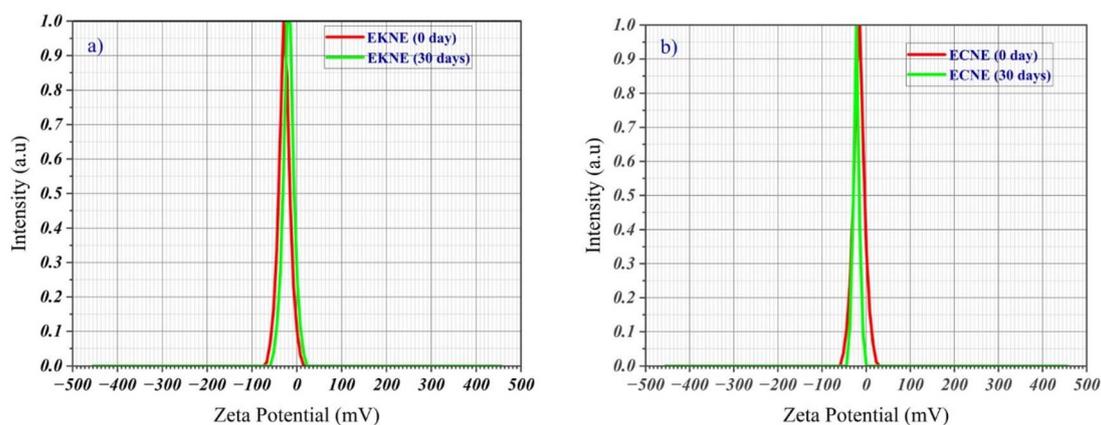
Fig. 6 Zeta potential values of (a) *E. kachinensis* nanoemulsion and (b) *E. ciliata* nanoemulsion.

kachinensis nanoemulsion and 0.336 to 0.231 for the *E. ciliata* nanoemulsion, indicating greater uniformity in droplet size distribution. This trend is consistent with changes in droplet size, which may be attributed to electrostatic repulsion among particles. Similarly, the zeta potential values also decreased from -27.8 to -20.1 mV for the *E. kachinensis* nanoemulsion and from -11.2 to -7.9 mV for the *E. ciliata* nanoemulsion. Previous reports have demonstrated similar changes in the droplet size, PDI and zeta potential values of a nanoemulsion formulated from citrus[38] and *Cymbopogon nardus*[39] essential oils. Based on the above analysis, the nanoemulsion maintained good stability during storage time.

FTIR spectroscopy was used to identify the characteristic functional groups of the essential oils and investigate the interactions between the essential oils, water, and surfactant by measuring the absorption peaks. As seen in Fig. 7, the spectra exhibited the characteristic peaks of Tween 80, *E. kachinensis*, and *E. ciliata* essential oils, respectively, without the appearance of any new peaks.

The FTIR spectra of *E. kachinensis* nanoemulsion presented characteristic peaks at 3447, 1738, 1645, 1045 and 1089 cm^{-1}, corresponding to the stretching vibrations of O–H, C=O and

C–O groups, which are typical groups found in *E. kachinensis* essential oils and Tween 80. However, the intensity of the O–H peak and its broad band at 3447 cm^{-1} compared with the FTIR spectrum of *E. kachinensis* essential oils and Tween 80 can be due to the presence of a water phase. Furthermore, the presence of characteristic functional groups of the essential oils in the nanoemulsion suggested that the components of the essential oils were retained during the nanoemulsion formation process. The analysis of *E. ciliata* nanoemulsion yields similar results to that of *E. kachinensis* nanoemulsion. This result indicated that Tween 80 played the role as a surfactant, and no chemical interactions occurred between this compound and essential oils.

The mechanism of nanoemulsion formation can be proposed as follows. Tween 80, a non-ionic surfactant with a hydrophilic head and a lipophilic tail, functions to reduce interfacial tension between the essential oils and water. Initially, the hydrophobic tail of Tween 80 adheres to the oil droplets. With the addition of the aqueous phase, the hydrophilic head of Tween 80 interacts with water. As the interfacial tension between the oils and water phase decreases, mechanical processes, such as stirring and ultrasonication, cause the oil
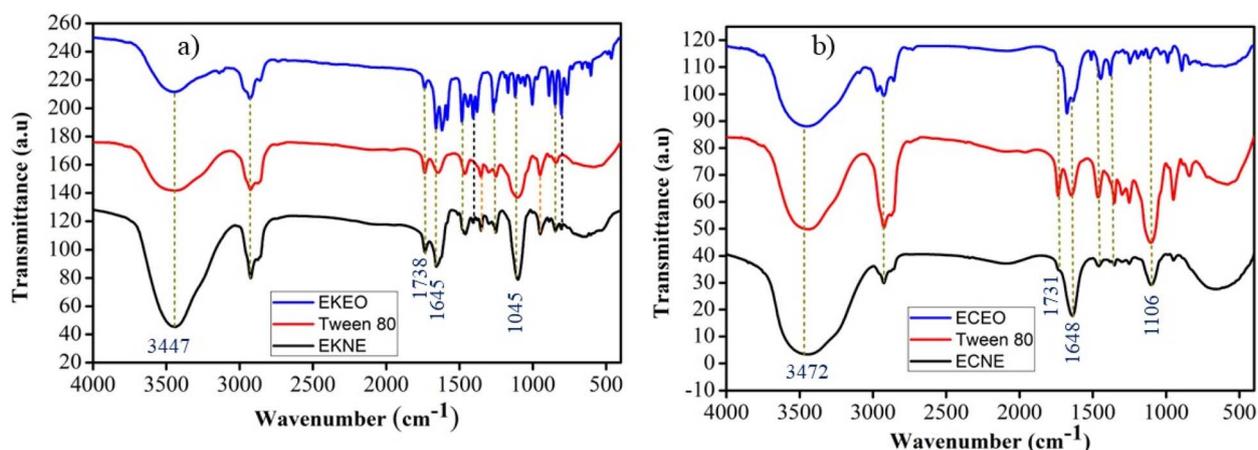

Fig. 7 FTIR spectra of the essential oils, nanoemulsions and Tween 80: (a) *E. kachinensis*, (b) *E. ciliata*.

droplets to break into smaller droplets. These smaller oil droplets are then stabilized by a layer of Tween 80, which creates both electrostatic and steric repulsion, preventing the coalescence of these droplets into larger ones, thereby stabilizing the emulsion system.

Molecular activity is key to determining the chemical properties and structural positions during chemical reactions.[40–42] The interactions of compounds can be significantly influenced by the distribution of atomic charges. The measurement of localized reactive regions is important because it enables the interpretation of reactive variations due to different atomic positions in a molecule.[43,44] This information can be obtained from Mulliken atomic charges.[43] Before calculating Mulliken atomic charges, the molecular structures of compounds, including Tween 80, dehydroelsholtzia ketone, *trans*-β-ocimene and β-farnesene, were optimized, as shown in Fig. 8. Mulliken atomic charges of Tween 80, dehydroelshotzia ketone, *trans*-β-ocimene and β-farnesene were analyzed and are listed in Tables S1–S4† and depicted in Fig. 9a–d. The atomic charges of Tween 80 revealed that all hydrogen atoms had a positive charge; however, H67, H68, and H71 possessed a higher positive charge (from 0.390958 to −0.394601) than the other hydrogen atoms. These hydrogen atoms attack oxygen atoms and can form hydrogen bonds with other molecules. Among the carbon atoms, C36 (0.62954) had the highest positive charge, while C42 (−0.4413) had the highest negative charge. Furthermore, the charge distribution on the oxygen atoms (O6, O7, O8) indicated that these sites exhibited higher electron density (from

−0.60662 to −0.60842), suggesting their potential as proton acceptors. The Mulliken atomic charge analysis of dehydroelsholtzia ketone demonstrated that two oxygen atoms (O1 and O2) had significant negative charges (−0.45101 and −0.52453), rendering them capable of forming hydrogen bonds with H67, H68, and H71 of Tween 80. As a result, this compound is effectively stabilized in aqueous environments through hydrogen bonding interactions with Tween 80.

Additionally, carbon atoms C9 (−0.50462), C11 (−0.51198), and C12 (−0.53255) exhibited strong negative charges, indicating hydrophobicity. Consequently, the hydrophobic segment of Tween 80 may encapsulate these regions, thereby enhancing the solubility of dehydroelsholtzia ketone in the aqueous phase. This encapsulation prevents phase separation and aggregation, ensuring stable dispersion of the compound within the emulsion system. Meanwhile, the Mulliken atomic charges of the principal components in *E. ciliata*, such as *trans*-β-ocimene and β-farnesene, revealed that both molecules contained negatively charged carbon atoms. Among the carbon atoms, C6, C7, and C8 in *trans*-β-ocimene and C8, C11, and C12 in β-farnesene had higher negative charges. These hydrophobic regions exhibited a strong tendency to be encapsulated by Tween 80 *via* van der Waals interactions, further contributing to the stabilization of these compounds within the emulsion system. As a result, dehydroelsholtzia ketone, the main component of *E. kachinensis* essential oils, interacts more effectively with both the hydrophilic and lipophilic regions of Tween 80 *via* hydrogen bonds and van der Waals interaction, further contributing to the better
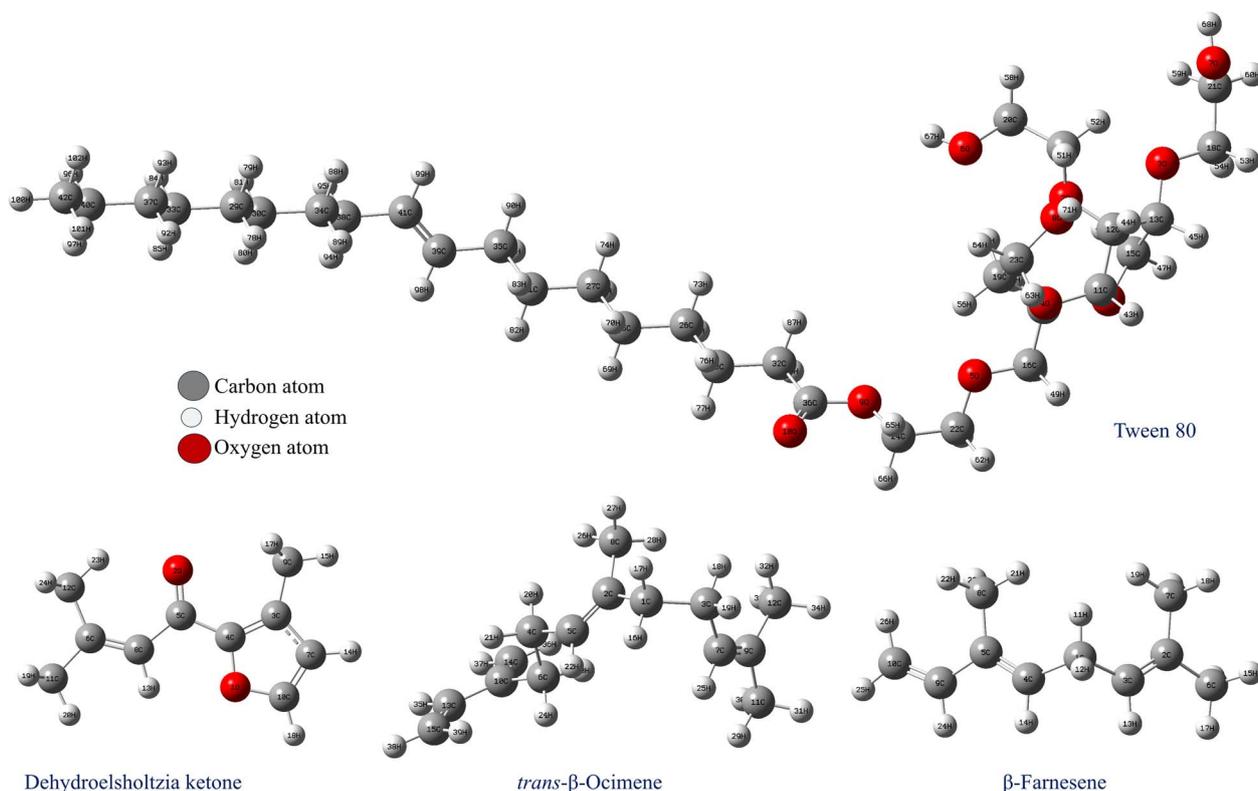

Fig. 8 Optimized molecular structures of Tween 80, dehydroelsholtzia ketone, *trans*-β-ocimene and β-farnesene.
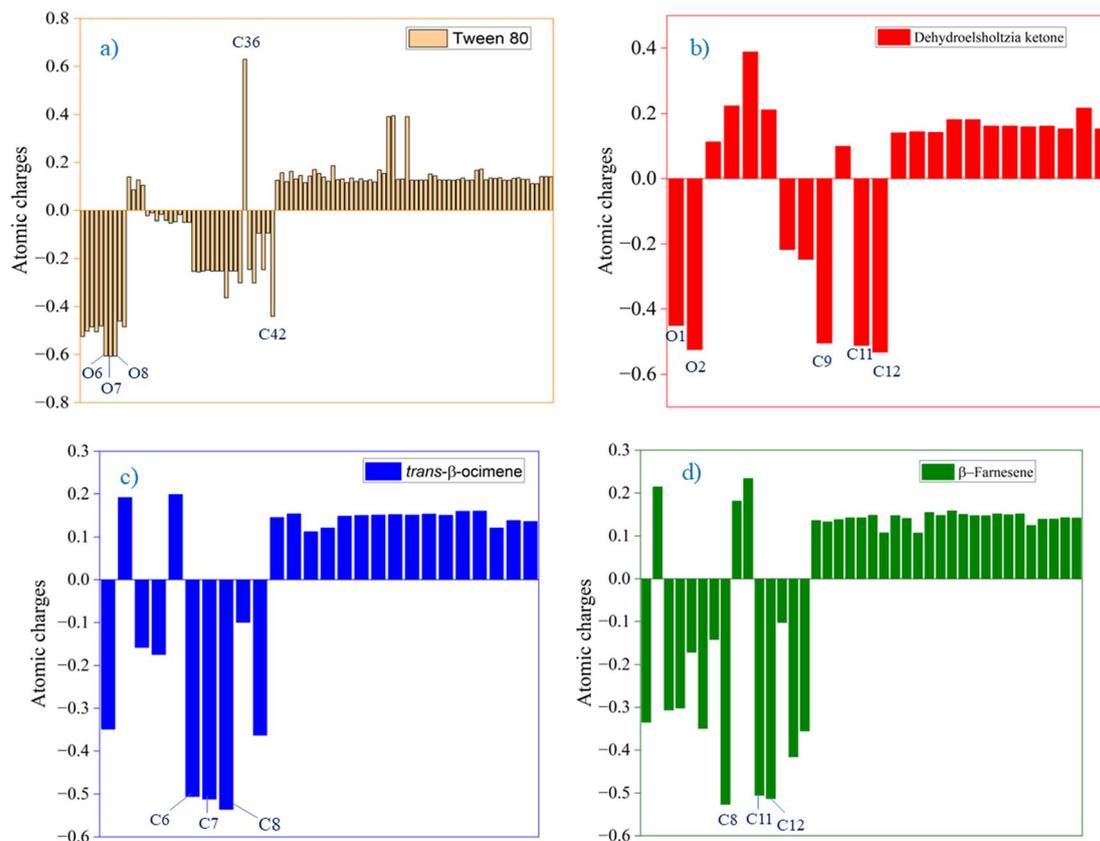
Fig. 9 Mulliken atomic charges of (a) Tween 80, (b) dehydroelsholtzia ketone, (c) *trans*-β-ocimene and (d) β-farnesene.

stabilization of these compounds within the emulsion system than *trans*-β-ocimene and β-farnesene in *E. ciliata* essential oils. These results explain that the *E. kachinensis* nanoemulsion was more stable, with a higher absolute zeta potential value than the *E. ciliata* nanoemulsion.

3.3 Antibacterial activity of the *E. kachinensis* and *E. ciliata* nanoemulsions

To the best of our knowledge, there is no previous report on the antibacterial activity of nanoemulsions of *E. kachinensis* and *E.

ciliata essential oils. Therefore, for the first time, their antibacterial activities are reported here. The agar disc diffusion method revealed their effective inhibition of the two tested bacterial strains, namely *P. aeruginosa* and *S. aureus* (Fig. 10). The inhibition zone diameters were 12.0 ± 0.3 and 14.0 ± 0.2 mm for the *E. ciliata* essential oil, 14.3 ± 0.3 and 15.5 ± 0.1 mm for its nanoemulsion, 11.2 ± 04 and 12.5 ± 0.2 mm for the *E. kachinensis* essential oil, and 13.8 ± 04 and 15.0 ± 04 mm for its nanoemulsion. In comparison, ciprofloxacin displayed inhibition zones of 12.0 ± 0.2 and 15.2 ± 0.3 mm against *P.*
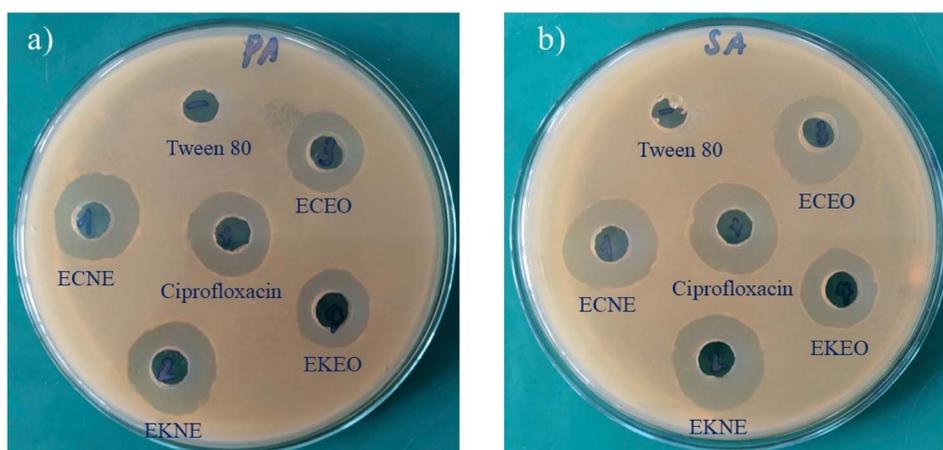

Fig. 10 Antibacterial activity of *E. kachinensis* and *E. ciliata* essential oils and their nanoemulsions against (a) *P. aeruginosa* and (b) *S. aureus*.

Table 2 Antibacterial activity of the *E. kachinensis* and *E. ciliata* nanoemulsions ($n = 3$)

Bacteria	MIC values (mg mL^{-1})					MIC values (µg mL^{-1})
	E. kachinensis essential oil	*E. kachinensis* nanoemulsion	*E. ciliata* essential oil	*E. ciliata* nanoemulsion	Tween 80	Ciprofloxacin
E. coli	0.9375 ± 0.0000	0.6250 ± 0.2706	0.9375 ± 0.0000	0.4688 ± 0.0000	3.7500 ± 1.8334	0.0156 ± 0.0000
P. aeruginosa	0.9375 ± 0.0000	0.7813 ± 0.2706	0.9375 ± 0.0000	0.7813 ± 0.2706	2.8125 ± 0.0000	0.1875 ± 0.0000
K. pneumoniae	0.6250 ± 0.2706	0.6250 ± 0.2706	0.4688 ± 0.0000	0.3125 ± 0.1353	2.8125 ± 0.0000	0.5000 ± 0.0000
S. aureus	1.8750 ± 0.0000	0.9375 ± 0.0000	0.3906 ± 0.1353	0.1503 ± 0.0677	5.6250 ± 0.0000	0.2500 ± 0.0000
B. subtilis	0.7810 ± 0.2706	0.625 ± 0.2706	0.1953 ± 0.0677	0.0372 ± 0.0136	4.6875 ± 1.6231	0.0625 ± 0.0000
S. epidermidis	0.9375 ± 0.000	0.625 ± 0.2706	0.3906 ± 0.1105	0.0743 ± 0.0371	2.8125 ± 0.0000	0.1250 ± 0.0000

aeruginosa and *S. aureus*, respectively, while Tween (15%) exhibited no antibacterial activity. These results indicate that the nanoemulsions of both essential oils possessed enhanced antibacterial efficacy against the tested strains compared with their corresponding essential oils. Similar results have been reported in previous studies.[45,46]

The results of the antibacterial activity of the samples based on the broth microdilution method are provided in Table 2 and Fig. 11. In general, both nanoemulsions had MIC values in the range of 0.0037 to 1.8750 mg mL^{-1} and were found to have a greater inhibitory effect on bacteria than their corresponding essential oils. Our findings are in accordance with previous antibacterial results of nanoemulsions prepared from thyme,[47] Sichuan pepper,[48] sage,[49] *Lavandula intermedia*[50] and garlic essential oils.[12] Similarly, the nanoemulsion of laurel essential oil was more effective against *Staphylococcus aureus* and *Enterococcus faecalis* than laurel essential oils itself.[27] In addition, these results show that the essential oil and nanoemulsion of *E. kachinensis* were more effective against Gram-negative

bacteria than Gram-positive. Moreover, the inhibitory effect of *E. kachinensis* essential oil collected from Cao Bang, Vietnam on *E. coli* and *P. aeruginosa* was better than that collected from Guizhou, China.[51] The MIC value of the *E. kachinensis* essential oil collected from Guizhou, China against both *E. coli* and *P. aeruginosa* was 1.3 mg mL^{-1}. However, its effect on *S. aureus* and *B. subtilis* was lower, with MIC values of 0.64 and 0.32 mg mL^{-1}, respectively.[51] This difference in antibacterial activity is possible because of the composition of essential oil components and their quality. Meanwhile, the essential oil and nanoemulsion of *E. ciliata* exhibited more effective antibacterial activity against Gram-positive bacteria than Gram-negative bacteria. Especially, the essential oil and nanoemulsion of *E. ciliata* provided the best activity against *S. aureus*, with MIC values of 0.625 and 0.0372 mg mL^{-1}, respectively. According to Tian 2013, *E. ciliata* essential oil collected from China showed strong inhibitory activity against *S. aureus*, *B. subtilis* and *E. coli*, with MIC values of 6.88, 0.02 and 1.08 µL mL^{-1}, respectively.[52] Besides, findings from previous studies indicate that Tween 80 might reduce the
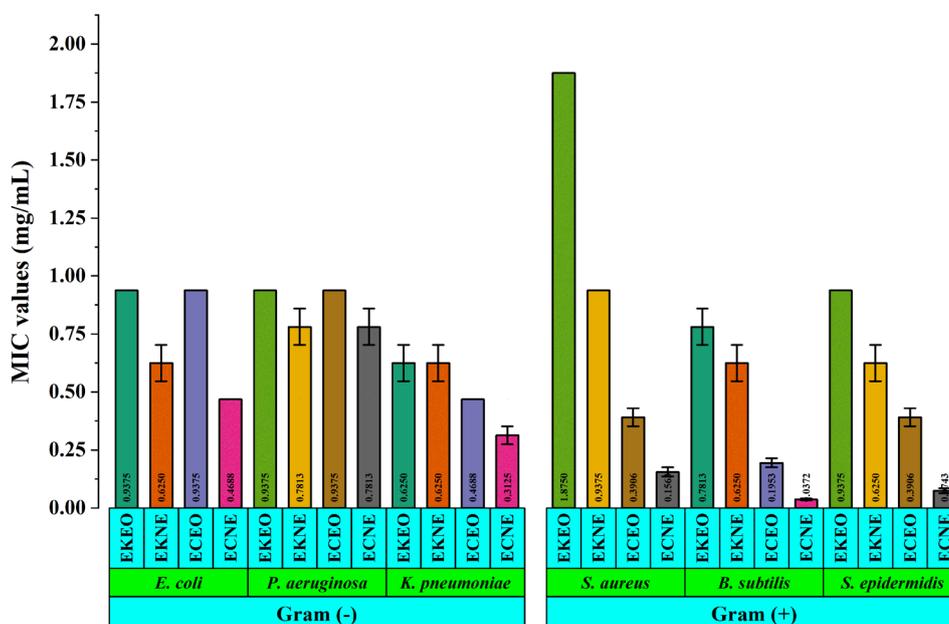

Fig. 11 Antibacterial activity of the *E. kachinensis* and *E. ciliata* essential oils and their nanoemulsions ($n = 3$, error bars show the standard deviations).

antibacterial efficacy of antibacterial agents, such as nanoemulsions.[53,54]

The results also showed a significant correlation between the concentration of Tween 80 in the nanoemulsions and their antibacterial effects. These findings emphasized the necessity for optimizing the Tween 80 concentration in these nano-emulsion formulations to maximize their antimicrobial effectiveness while maintaining stability. When only 15% Tween 80 was used, the antibacterial activity of the nanoemulsions did not change much, with MIC values remaining ≥ 2.8125 mg mL^{-1}, proving no obvious side effects of 15% Tween 80 on the activity of the nanoemulsions. This finding is similar to that reported by Hou.[55] Ciprofloxacin was used as the standard control in this study, and it was found to be highly active in comparison with the nanoemulsions.

3.4 Anticancer activity against HepG2 liver cancer cells

Although there have been some reports on the anticancer properties of essential oils or extracts from certain species of the *Elshotzia* genus, studies on nanoemulsions synthesized from these species, as well as their activity, are still limited.

The effects of the essential oils and their nanoemulsions of two species belonging to the *Elshotzia* genus (*i.e.*, *E. kachinensis* and *E. ciliata*) on HepG2 liver cancer cell morphology are shown in Fig. 12a–d. Fig. 12a demonstrates that at concentrations ranging from 10 to 50 μg mL^{-1}, the *E. kachinensis* essential oil had minimal effects on cell density and morphology. At higher

concentrations (100 to 500 μg mL^{-1}), large gaps appeared, indicating that the essential oil reduced the cell proliferation capacity, while some dark-colored dead cells, which were not adherent to the culture plate surface, were observed. When cells were treated with the *E. kachinensis* essential oil nanoemulsion (Fig. 12b), a significant reduction in cell density was observed at concentrations ≥ 50 μg mL^{-1}, and the appearance of dead cells was noted at concentrations ≥ 100 μg mL^{-1}. The impact of the *E. ciliata* essential oil on HepG2 liver cancer cell morphology (as shown in Fig. 12c) was evident at concentrations above 50 μg mL^{-1}, while the nanoemulsion of *E. ciliata* essential oil caused a noticeable reduction in cell density even at 10 μg mL^{-1}. The nanoemulsion of *E. ciliata* essential oil (Fig. 12d) also led to the appearance of dead cells at concentrations as low as 50 μg mL^{-1}. A quantitative analysis of the ability of the essential oils and nanoemulsions to inhibit cell proliferation is illustrated in Fig. 13a and b.

As seen in Fig. 13a, the nanoemulsion of *E. kachinensis* essential oil caused cell inhibition ranging from 20% to 80%, which was significantly higher than that elicited by the *E. kachinensis* essential oil at each concentration ($p < 0.05$). The IC$_{50}$ values were determined to be 84.3 μg mL^{-1} for the *E. kachinensis* nanoemulsion and greater than 200 μg mL^{-1} for the *E. kachinensis* essential oil. Similar results are also given in Fig. 13b; the inhibition percentage of the *E. ciliata* essential oil ranged from 7% to 65%, while the inhibition percentage of the *E. ciliata* nanoemulsion ranged from 25% to 80% ($p < 0.05$). The
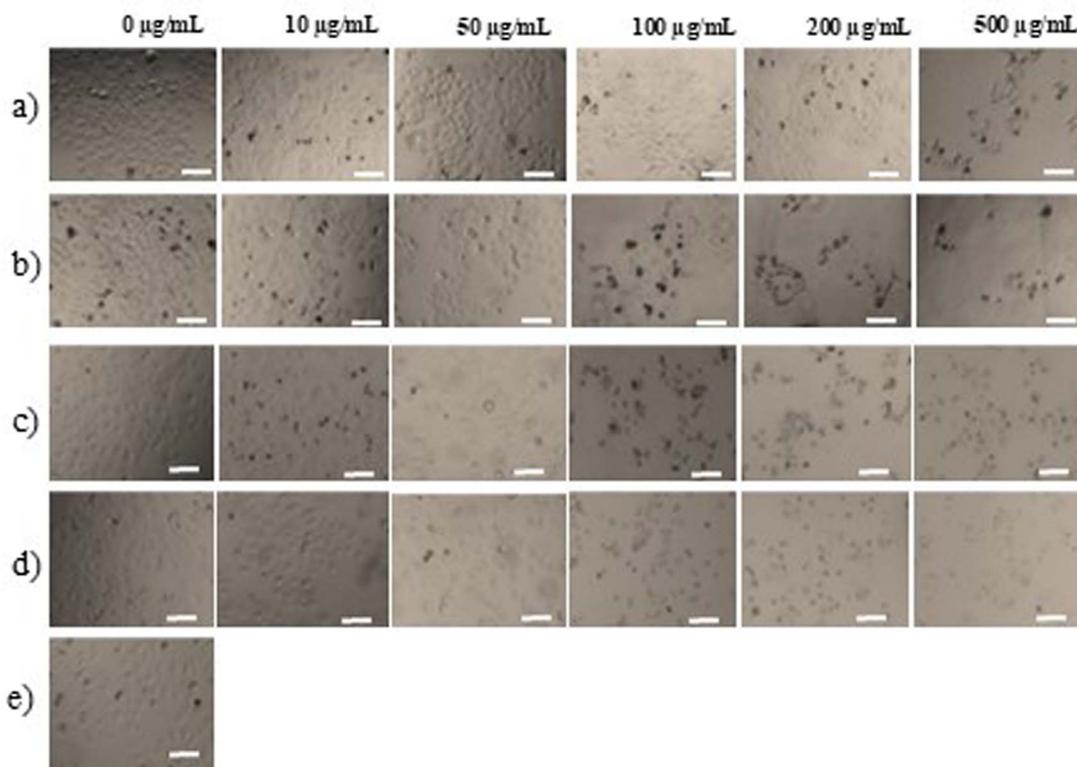

Fig. 12 Changes in the cell morphology and proliferation of HepG2 liver cancer cells under the treatment of (a) *E. kachinensis* oil, (b) *E. kachinensis* nanoemulsion; (c) *E. ciliata* oil (d) *E. ciliata* nanoemulsion, and (e) 5-FU. Mann–Whitney test; scale bar = 50 μm.
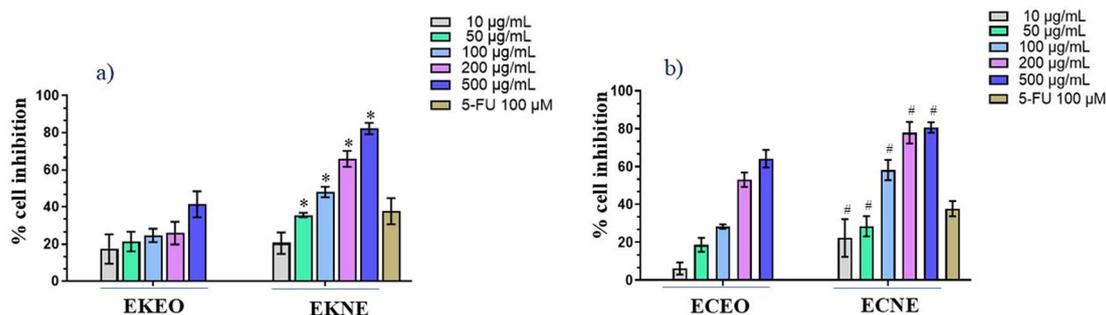
Fig. 13 Inhibitory effects of the (a) *E. kachinensis* essential oil and *E. kachinensis* nanoemulsion and (b) *E. ciliata* essential oil and *E. ciliata* nanoemulsion on HepG2 cell proliferation. *$p < 0.05$ versus* EKEO and ECEO; #$p < 0.05$ *versus* EKNE and ECNE, Mann–Whitney test.

IC_{50} values were determined to be 72.1 μg mL^{-1} for the *E. ciliata* nanoemulsion and 163.7 μg mL^{-1} for the *E. ciliata* essential oil. Thus, both nanoemulsions exhibited significantly stronger inhibitory effects than the corresponding essential oils. Meanwhile, in this cell line, 5-FU demonstrated IC_{50} values ranging from 117 to 128 μM. At a concentration of 100 μM, 5-FU achieved an approximate inhibition rate of 40%, which provides a sufficiently distinct reference point for comparative analysis with the nanoemulsions. Previous studies have indicated the anticancer activity of the *Elshotzia* genus against human glioblastoma, pancreatic cancer, and breast cancer.[56] The nanoemulsion of *Pinus morrisonicola* essential oil with a droplet size of 41.1 nm and polydispersion index of 0.31 showed a stronger inhibitory effect on cancer cells than normal cells (HFF).[17] Additionally, the nanoemulsion exhibited effective antioxidant activity by inhibiting ABTS and DPPH free radicals with IC_{50} values of 4 and 40 μg mL^{-1}, respectively.[17] In this study, we demonstrate that essential oils from *E. ciliata* and *E. kachinensis* could inhibit the proliferation of HepG2 liver cancer cells. Manaa reported that a nanoemulsion of oregano essential oil exhibited significantly reduced IC_{50} values against the A549 cell line compared with the free essential oil.[57] Thus, the results from this study propose that using nanoemulsion form is an effective strategy for enhancing the anti-cancer efficacy of essential oils.

4 Conclusion

Nanoemulsions were successfully prepared from *E. kachinensis* and *E. ciliata* essential oils using ultrasonic homogenization in an aqueous medium containing Tween 80 as the surfactant. The prepared nanoemulsions exhibited good stability and droplet sizes in the nanoscale (*i.e.*, 72.81 and 32.13 nm). In addition, the *E. kachinensis* nanoemulsion displayed better size distribution, PDI < 0.3 and better stability than the *E. ciliata* nanoemulsion. The Mulliken atomic charge analysis explained that the *E. kachinensis* nanoemulsion was more stable than the *E. ciliata* nanoemulsion. However, the nanoemulsion of *E. ciliata* displayed stronger antibacterial activity and anticancer activity than the nanoemulsion of *E. kachinensis*. Both nanoemulsions exhibited significantly higher antibacterial and anticancer activities than the corresponding essential oils, indicating the

advantages of nanoemulsions. Based on the results of this study, we also propose that the development of an efficient and safe delivery system holds significant potential in advancing the utilization of essential oils for antibacterial and anticancer activities.

Data availability

The datasets produced and analyzed during this study are available from the corresponding author upon reasonable request.

Author contributions

Nguyen Quang Tinh: conceptualization, investigation, writing-original draft; Dang Van Thanh: conceptualization, resource, editing, Nguyen Van Thu: data curation, methodology, formal analysis, Bui Thi Quynh Nhung: resource, methodology, investigation, Pham Ngoc Huyen: conceptualization, investigation, data curation, Nguyen Phu Hung: formal analysis, writing-review, Nguyen Thi Thuy: formal analysis, validation and editing, Pham Dieu Thuy: data curation, methodology, formal analysis, Nguyen Hoa Mi: software, visualization, formal analysis, Khieu Thi Tam: conceptualization, resource, writing and editing.

Conflicts of interest

There are no conflicts to declare.

Notes and references

1 Z. Guo, Z. Liu, X. Wang, W. Liu, R. Jiang, R. Cheng and G. She, *Chem. Cent. J.*, 2012, **6**, 1–8.

2 A.-L. Liu, S. M. Lee, Y.-T. Wang and G.-H. Du, *J. Chin. Pharm. Sci.*, 2007, **16**, 73.

3 L. Pudziuvelyte, M. Stankevicius, A. Maruska, V. Petrikaite, O. Ragazinskiene, G. Draksiene and J. Bernatoniene, *Ind. Crops Prod.*, 2017, **107**, 90–96.

4 T. Sripahco, S. Khruengsai, R. Charoensup, J. Tovaranonte and P. Pripdeevech, *Sci. Rep.*, 2022, **12**, 2225.

5 J. Liang, Y. Shao, H. Wu, Y. An, J. Wang, J. Zhang and W. Kong, *Foods*, 2021, **10**, 2304.

6 P. N. Paudel, P. Satyal, W. N. Setzer, S. Awale, S. Watanabe, J. Maneenet, R. Satyal, A. Acharya, M. Phuyal and R. Gyawali, *Nat. Prod. Commun.*, 2023, **18**, 1934578X231189325.

7 S. Chen, J. Chen, Y. Xu, X. Wang and J. Li, *J. Ethnopharmacol.*, 2022, **297**, 115549.

8 J.-W. Zhang, Y.-X. Feng, Y.-S. Du, X.-X. Lu, Y. Zheng, W. Dan and S.-S. Du, *J. Oleo Sci.*, 2022, **71**, 1075–1084.

9 F. Li, C. Wang, J. Xu, X. Wang, M. Cao, S. Wang, T. Zhang, Y. Xu, J. Wang and S. Pan, *Front. Microbiol.*, 2023, **14**, 1219004.

10 J. Mendes, H. Martins, C. Otoni, N. Santana, R. Silva, A. Da Silva, M. Silva, M. Correia, G. Machado and A. Pinheiro, *LWT*, 2018, **93**, 659–664.

11 Z. Lou, J. Chen, F. Yu, H. Wang, X. Kou, C. Ma and S. Zhu, *Lwt*, 2017, **80**, 371–377.

12 M. Liu, Y. Pan, M. Feng, W. Guo, X. Fan, L. Feng, J. Huang and Y. Cao, *Ultrason. Sonochem.*, 2022, **90**, 106201.

13 X. Fu, Y. Gao, W. Yan, Z. Zhang, S. Sarker, Y. Yin, Q. Liu, J. Feng and J. Chen, *RSC Adv.*, 2022, **12**, 3180–3190.

14 A. Gupta, H. B. Eral, T. A. Hatton and P. S. Doyle, *Soft Matter*, 2016, **12**, 2826–2841.

15 D. Renggli and P. S. Doyle, *Soft Matter*, 2025, **21**, 652–669.

16 I. R. Singh and A. K. Pulikkal, *OpenNano*, 2022, **8**, 100066.

17 N. Khatamian, M. Soltani, B. Shadan, A. Neamati, M. H. Tabrizi and B. Hormozi, *Inorg. Nano-Met. Chem.*, 2022, **52**, 253–261.

18 A. B. Perumal, X. Li, Z. Su and Y. He, *Ultrason. Sonochem.*, 2021, **76**, 105649.

19 W. Wang, Z. Leng, Q. Liu, J. Zhao and S. Li, *Ind. Crops Prod.*, 2024, **219**, 118987.

20 R. P. Adams, *Identification of Essential Oil Components by Gas Chromatography/mass Spectrometry*, Allured Publishing Corporation Carol Stream, 2007.

21 M. D. Julian and R. Jiajia, *Crit. Rev. Food Sci. Nutr.*, 2011, **51**, 285–330.

22 T. P. Lazou and S. C. Chaintoutis, *J. Microbiol. Methods*, 2023, **204**, 106649.

23 S. Hussiny, A. Elissawy, O. Eldahshan, M. Elshanawany and A.-N. Singab, *Arch. Pharm. Sci. Ain Shams Univ.*, 2020, **4**, 207–214.

24 A. Russo, C. Formisano, D. Rigano, F. Senatore, S. Delfine, V. Cardile, S. Rosselli and M. Bruno, *Food Chem. Toxicol.*, 2013, **55**, 42–47.

25 M. Frisch, G. Trucks, H. Schlegel, G. Scuseria, M. Robb, J. Cheeseman, G. Scalmani, V. Barone, G. Petersson and H. Nakatsuji, *Gaussian 16*, Wallingford CT, 2016.

26 N. X. Dũng, L. Van Hac, L. H. Hái and P. A. Leclercq, *J. Essent. Oil Res.*, 1996, **8**, 107–109.

27 Y. Özogul, N. El Abed and F. Özogul, *Food Chem.*, 2022, **368**, 130831.

28 K. Fidyt, A. Fiedorowicz, L. Strządała and A. Szumny, *Cancer Med.*, 2016, **5**, 3007–3017.

29 S. S. Dahham, Y. M. Tabana, M. A. Iqbal, M. B. Ahamed, M. O. Ezzat, A. S. Majid and A. M. Majid, *Molecules*, 2015, **20**, 11808–11829.

30 S. A. Singh, Y. A. Potdar, R. S. Pawar and S. V. Bhat, *Nat. Prod. Commun.*, 2011, **6**, 1934578X1100600902.

31 S. Ben-Yehoshua and R. Ofir, 2009.

32 A. I. Hussain, F. Anwar, S. Rasheed, P. S. Nigam, O. Janneh and S. D. Sarker, *Rev. Bras. Farmacogn.*, 2011, **21**, 943–952.

33 O. Campolo, G. Giunti, M. Laigle, T. Michel and V. Palmeri, *Ind. Crops Prod.*, 2020, **157**, 112935.

34 R. Pathania, R. Kaushik and M. A. Khan, *Curr. Res. Nutr. Food Sci.*, 2018, **6**, 626–643.

35 O. Gul, F. T. Saricaoglu, A. Besir, I. Atalar and F. Yazici, *Ultrason. Sonochem.*, 2018, **41**, 466–474.

36 S. Kumari, R. Kumaraswamy, R. C. Choudhary, S. Sharma, A. Pal, R. Raliya, P. Biswas and V. Saharan, *Sci. Rep.*, 2018, **8**, 6650.

37 P. Pongsumpun, S. Iwamoto and U. Siripatrawan, *Ultrason. Sonochem.*, 2020, **60**, 104604.

38 Z. Kang, S. Chen, Y. Zhou, S. Ullah and H. Liang, *Innovative Food Sci. Emerging Technol.*, 2022, **80**, 103110.

39 N. Somala, C. Laosinwattana and M. Teerarak, *Sci. Rep.*, 2022, **12**, 10280.

40 O. Dagdag, A. El Harfi, L. El Gana, Z. S Safi, L. Guo, A. Berisha, C. Verma, E. E. Ebenso, N. Wazzan and M. El Gouri, *J. Appl. Polym. Sci.*, 2021, **138**, 49673.

41 O. Dagdag, Z. Safi, H. Erramli, N. Wazzan, L. Guo, C. Verma, E. Ebenso, S. Kaya and A. El Harfi, *Mater. Today Commun.*, 2020, **22**, 100800.

42 R. Ihamdane, M. Tiskar, B. Outemsaa, L. Zelmat, O. Dagdag, A. Berisha, E. Berdimurodov, E. E. Ebenso and A. Chaouch, *Arabian J. Sci. Eng.*, 2023, **48**, 7685–7701.

43 M. Manssouri, A. Chraka, I. Raissouni, A. Wahby and N. EL Aouad, *Anal. Bioanal. Electrochem.*, 2024, **16**, 507–536.

44 R. Solmaz, G. Kardaş, M. Çulha, B. Yazıcı and M. Erbil, *Electrochim. Acta*, 2008, **53**, 5941–5952.

45 R. Moghimi, L. Ghaderi, H. Rafati, A. Aliahmadi and D. J. McClements, *Food Chem.*, 2016, **194**, 410–415.

46 E. Fachriyah, P. Wibawa and A. Awaliyah, *J. Phys.: Conf. Ser.*, 2020, **1524**, 012060.

47 Y. Ozogul, E. K. Boğa, I. Akyol, M. Durmus, Y. Ucar, J. M. Regenstein and A. R. Köşker, *Food Biosci.*, 2020, **36**, 100635.

48 Y. Shi, M. Zhang, K. Chen and M. Wang, *Lwt*, 2022, **154**, 112779.

49 H. Yazgan, *Lwt*, 2020, **130**, 109669.

50 S. Garzoli, S. Petralito, E. Ovidi, G. Turchetti, V. L. Masci, A. Tiezzi, J. Trilli, S. Cesa, M. A. Casadei and P. Giacomello, *Ind. Crops Prod.*, 2020, **145**, 112068.

51 C. F. Zhu, W. D. Ping, Y. Z. Chang, L. C. Ming, M. Lin and Y. X. Sheng, *Guihaia*, 2012, **32**, 269–273.

52 G.-h. Tian, *Chin. Herb. Med.*, 2013, **5**, 104–108.

53 Q. Ma, P. M. Davidson and Q. Zhong, *Int. J. Food Microbiol.*, 2016, **226**, 20–25.

54 S. Mansouri, M. Pajohi-Alamoti, N. Aghajani, B. Bazargani-Gilani and A. Nourian, *J. Sci. Food Agric.*, 2021, **101**, 3880–3888.

55 K. Hou, Y. Xu, K. Cen, C. Gao, X. Feng and X. Tang, *Food Biosci.*, 2021, **43**, 101232.

56 F. Wang, X. Liu, Y. Chen, Y. An, W. Zhao, L. Wang, J. Tian, D. Kong, Y. Xu and Y. Ba, *Molecules*, 2022, **27**, 6411.

57 A. O. Manaa, H. H. Baghdadi, N. A. El-Nikhely, L. A. Heikal and L. S. El-Hosseiny, *J. Drug Delivery Sci. Technol.*, 2022, **78**, 103978.